BMC Biotechnology

RESEARCH

Open Access

Aripiprazole-loaded niosome/chitosan-gold nanoparticles for breast cancer chemo-photo therapy

Sajjad Alimohammadvand[1,2], Masoumeh Kaveh Zenjanab[1], Parvin Samadi Pakchin[1], Elaheh Dalir Abdolahinia[1,3], Jaleh Barar[4], Yadollah Omidi[4], Mohammad M. Pourseif[1,5,6], Marziyeh Fathi[1*] and Jalal Shayegh[7*]

Abstract

Introduction Breast cancer, a formidable global health challenge for women, necessitates innovative therapeutic strategies with enhanced efficacy and minimal side effects. Aripiprazole (ARI), a widely used schizophrenia medication, exhibits promising potential in the treatment of breast cancer. As cancer therapy evolves towards a combination approach, multimodal nano-based delivery systems, such as ARI-loaded niosomes (NIOs) combined with Chitosan-Au nanoparticles for chemo-photothermal therapy, show promise over traditional chemotherapy alone by enhancing targeted efficacy and minimizing side effects.

Methods In this study, a niosomal formulation was designed, incorporating ARI and chitosan-coated AuNPs (i.e. NIOs/AuNPs-CS/ARI), to study the synergistic effect of photothermal/chemotherapy in breast cancer cells.

Results The nanosystems were characterized using UV-Vis spectroscopy and Fourier-transform infrared spectroscopy (FT-IR), confirming the successful synthesis steps. The hydrodynamic diameter of NIOs/AuNPs-CS was determined to be 44.62 nm with a zeta potential of -0.836. Also, Transmission Electron Microscopy (TEM) and Field-Emission Scanning Electron Microscopical (FE-SEM) analysis were performed to assess the size and morphology of NPs. The loading efficiency of ARI in NIOs and NIOs/AuNPs–CS was 75% and 88%, respectively. Furthermore, the release rate of the drug from NIOs/AuNPs–CS is higher than blank NIOs at two pH values (5.8 and 7.4). The cellular uptake of AuNPs-CS-encapsulated NIOs was considerably higher than that of blank NIOs. The Annexin V/PI staining assay showed that the apoptosis/necrosis rate was high in NIOs/AuNPs-CS/ARI (46%) and NIOs/ARI (36%) in 48 h. The results of MTT assessments demonstrated higher cytotoxicity by ARI-loaded NPs. The viability of MCF-7 cells treated with NIOs/AuNPs-CS/ARI was reduced from 60% and 50% to 40% and 20%, respectively, after 24 and 48 h upon laser irradiation.

Conclusion The results of this experiment demonstrated the remarkable effectiveness of NIOs/AuNPs-CS/ARI in cancer treatment, owing to their unique properties, including the PTT capability and pH sensitivity.

Keywords Niosomes, Aripiprazole, Photothermal therapy, Combination therapy, Breast cancer, Chitosan, Gold nanoparticles

*Correspondence:
Marziyeh Fathi
fathi.marziyeh@yahoo.com; fathim@tbzmed.ac.ir
Jalal Shayegh
jalalshayegh@gmail.com

Full list of author information is available at the end of the article

Introduction

Breast cancer is the most common and life-threatening cancer in females worldwide [1]. Despite having distinct subtypes, breast cancer cells differ significantly from healthy cells. For example, some receptors are highly expressed in cancerous cells that control fundamental cellular functions such as proliferation, adhesion, differentiation, and survival [2, 3]. Additionally, their distinct metabolic mechanisms result in an altered tumor microenvironment (e.g. hypoxia and acidic extracellular pH) [4]. Although surgery and chemotherapy hold great promise in breast cancer therapy, the efficacy is suboptimal due to side effects -including severe nausea, hair loss, and fatigue [5]- as well as the development of resistance by cancer cells. Cancer cells can acquire genetic mutations that modify the drug target, reducing drug binding, and efficacy. These mutations can alter the target structure, making it difficult for the drug to exert its intended effect [6]. The new treatment modalities have attracted much attention and offer attractive and more effective alternatives to combat this disease. Several fields, including biomedicine, have witnessed an increase in nanotechnology research, applying nanoparticles (NPs) for cancer treatment [7]. Nanoparticle-based drug delivery has emerged as a promising cancer therapy approach [8]. This technology offers distinct advantages, such as targeted delivery, improved drug solubility [5], the ability to overcome drug resistance, and controlled release [9].

Among various NP-based delivery systems, niosomes (NIOs) are considered suitable platforms due to their biocompatibility, low toxicity, and facile synthesis [10]. They are vesicular nanocarriers and suitable for carrying both hydrophilic and hydrophobic drugs, being regarded as viable alternatives to liposomal [11, 12].

Moreover, a hybrid system of combination therapy, using photothermal therapy (PTT) and chemotherapy, is reported to be more effective due to the synergistic or complementary impacts of such an emerging combined treatment strategy [13].

PTT offers a localized, minimally invasive cancer therapy option, that uses a photothermal agent to convert light into heat to raise the temperature of the tumor site [14]. Gold nanoparticles (AuNPs) are one of the best photothermal agents that have photoacoustic and photothermal properties at specific wavelengths [15], leading to properties that make them attractive for hyperthermal therapy of cancer cells and for medical imaging [16, 17]. Near-infrared (NIR) laser is commonly employed in AuNPs-induced PTT as the optimal biological optical window, where the absorption by hemoglobin, melanin, and water is reduced, allowing deeper light penetration into fluids and tissues [18]. However, AuNPs must be stabilized for clinical applications to prevent aggregation in the biological milieu [19]. One approach for stabilizing AuNPs is surface modification, and encapsulation within chitosan (CS)-based NPs [20]. CS is a natural polysaccharide with abundant amine functional groups that offers unprecedented potential for the fabrication of multifunctional targeted/smart delivery systems [21]. In addition, it has been indicated that CS-stabilized AuNPs demonstrate improved biocompatibility and stability [20]. Due to the associated serious side effects, and resistance development with the customary chemotherapeutics, there has been a great interest in finding new alternatives, such as drug repurposing [22]. This strategy is gaining popularity among scientists as it offers a more viable and effective alternative to traditional drug discovery approaches [23]. In this regard, aripiprazole (ARI), a high-affinity partial agonist of the dopamine D2 receptor that is commonly used as an antipsychotic drug to treat schizophrenia [24], has attracted much attention. However, more recent studies have shown that ARI also has antiproliferative effects on different cancer cells, such as colon, gastric, and breast cancer cells in increased apoptosis [23]. ARI demonstrates a sensitization effect, especially in drug-resistant cancer cells and enhances radiosensitizing effects in various cancer cells [25, 26].

In this study, we aim to develop a multimodal nanosystem for the combination therapy of breast cancer. To this end, a niosomal formulation was proposed that encapsulates ARI as a chemotherapeutic agent, and AuNPs-CS for PTT therapy of breast cancer cells. This drug delivery system was engineered and characterized, utilizing physicochemical properties, encapsulation efficiency, and drug release properties in different conditions. The bioimpacts of NPs on breast cancer cells were studied by evaluating the cell uptake, cytotoxicity, and apoptosis/necrosis regulation. Further, the effectiveness of the chemo/PTT therapy combination of the synthesized NIOs/AuNPs-CS/ARI was investigated on MCF-7 cancer cells under laser irradiation.

Methods

Materials

Chloroauric acid ($HAuCl_4.\ 3H_2O$), chitosan (CS) (medium molecular weight), cholesterol, polysorbate 80 (Tween 80), and surfactant sorbitan monostearate (Span 60) were purchased from Sigma-Aldrich Corp (St. Louis, USA). Breast cancer cells (MCF-7) were purchased from the National Cell Bank of Iran, Pasteur Institute (Tehran, Iran). RPMI 1640 medium and FBS were prepared from Gibco, Invitrogen (Paisley, UK). The Annexin V-FITC kit for the detection of apoptosis/necrosis was provided by eBiosciences (MA, USA). Cell culture flasks and plates were purchased from SPL Life Science (South Korea).

Preparation of AuNPs-CS

The AuNPs-CS were synthesized according to our previously published method with slight modifications [27]. In this study, AuNPs-CS were prepared in lower concentrations of CS and $HAuCl_4$ solutions as well as lower temperature to achieve the smaller size of NPs. In brief, 50 mg of CS was dissolved in 10 mL acetic acid solution (1% v/v). Then 200 µL of $HAuCl_4$. $3H_2O$ (12.5 mM) was added dropwise to the CS solution under stirring conditions at 45 °C. After 3 h, the color of the solution was slowly changed from yellow to wine-red, which indicated the formation of AuNPs-CS. For purification, the obtained AuNPs-CS solution was centrifuged at 12,000 rpm for 10 min.

Synthesis of NIOs/AuNPs-CS, ARI-loaded NIOs, and ARI-loaded NIOs/AuNPs-CS

NIOs were synthesized using the thin-film hydration method [28]. Briefly, Span 60 (8 mg), Tween 80 (20 mg), cholesterol (4 mg), and ARI (4 mg) were dissolved in methanol (3 mL) and chloroform (3 mL). Then this solution was put in a rotary evaporator at 120 rpm and 60 °C for 1 h and the solvent was removed. The proniosomes were hydrated with 5 mL of PBS containing 500 µL of AuNPs-CS and the mixture was then subjected to probe sonication for 5 min in a pulsatile manner (50 s sonication with 10 s pause) with 30% amplitude to form ARI-loaded NIOs/AuNPs-CS (Fig. 1). The NIOs/AuNPs-CS, and NIOs/ARI were prepared using the same strategy, excluding the addition of ARI and AuNPs-CS during the synthesis procedure, respectively. The final solution was centrifuged at 12,000 rpm for 10 min at room temperature to remove the unreacted reagents.

Characterization of NIOs and NIOs/AuNPs-CS

The dynamic light scattering (DLS) Zetasizer Nano ZS (Malvern Instruments Ltd., Malvern, UK) was used to determine the zeta potential and size distribution of NIOs and NIOs/AuNPs-CS. The morphology of NIO was also analyzed using transmission electron microscopy (TEM). The sample was dispersed on copper grids at 1 mg/mL concentration without staining. LEO 906E TEM (Carl Zeiss, Oberkochen, Germany) with an accelerating voltage of 80 kV was used to image the TEM micrographs. Additionally, the morphology and size of the NPs were also determined using field-emission scanning electron microscopy (FE-SEM, S4160, Hitachi, Japan). The samples were spread on aluminum sheets, dried at 60 °C for 10 min, and then the sample was applied on the SEM stage under vacuum at 25 kv. The chemical structure of the synthesized nanosystems was investigated through Fourier-transform infrared spectroscopy (FT-IR) to verify the presence of specific chemical bonds and functional groups on the NPs. The FT-IR spectra were acquired in the 4000 –400 cm^{-1} range using KBr discs on an FT-IR Tensor 27 spectrometer (Bruker Optik GmbH, Ettlingen, Germany).

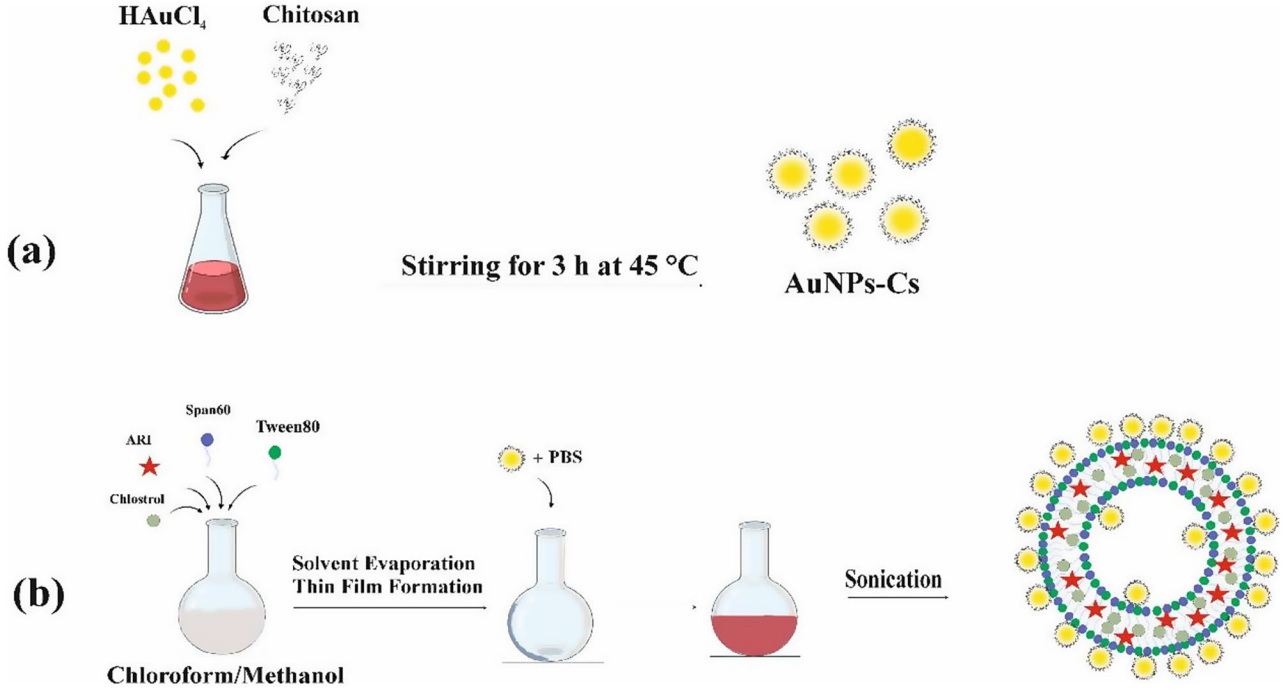

Fig. 1 Schematic representation of NIOs/AuNPs-CS/ARI synthesis. First, chitosan-coated AuNPs were prepared (**a**). NIOs were produced using solvent evaporation technique, loaded with AuNPs-CS and ARI to obtain final nanosystems, i.e. NIOs/AuNPs-CS/ARI (**b**)

Drug loading and in vitro releases

UV-Vis spectroscopy was used to determine the entrapment efficacy of ARI in the NIOs/AuNPs-CS. ARI-NIOs/AuNPs-CS was placed into the dialysis bag (12,000 Da) immersed in 100 mL PBS (pH=7.4) and stirred (4 °C, 30 min). The concentration of encapsulated ARI was then measured using UV-Vis spectroscopy at 250 nm. The following formula was used to calculate the efficiency of drug encapsulation (DE).

$$\mathrm{DE}\% = \frac{\text{initial drug concentration} - \text{unload drug concentration}}{\text{initial drug concentration}} \times 100$$

The release of ARI from NIOs and NIOs/AuNPs-CS was evaluated at pH=7.4 and 5.8. For this purpose, NPs were placed in the dialysis bag immersed in 100 mL PBS and agitated on a shaker (90 rpm and 37 °C). At predetermined time intervals, 2 mL of PBS was withdrawn and replaced with an equal volume of fresh PBS. The amount of ARI released was measured at 250 nm and calculated using the following equation:

$$\text{The amount of drug release } (\%) = \frac{C_i V_t + \sum_{i=1}^{n} (C_{i-1} V_s)}{m_t} \times 100$$

Where Ci represents the concentration of the drug release at time t, Vt represents the volume of the environment in which the drug is released, Vs represents the volume extracted from the release medium, and m_t represents the mass of the loaded ARI. A variety of mathematical models were used to determine the drug kinetics of ARI-NIOs/AuNPs-CS and NIOs/ARI at normal and acidic pH, including Zero-order, First order, Higuchi, Power law, Square root of mass, Hixson, Crowell, Three seconds' root of mass, Weibull, and Reciprocal.

Cellular uptake

The cellular uptake of NIOs and NIOs/AuNPs-CS by MCF-7 cells was investigated. First, NIOs and NIOs/AuNPs-CS were labeled by FITC, to this end, they were incubated with FITC (4 mg/mL methanol), overnight with continuous shaking at 4 °C. MCF-7 cells were seeded in six-well plates with a density of 5×10^5 cells/well. After 24 h, the cells were treated with FITC-labeled NPs (48 µM). An untreated group was included as a control, where cells were treated with PBS. After 4 h, the cells were washed with PBS, trypsinized, and centrifuged at 160 g for 5 min. Finally, NIOs and NIOs/AuNPs-CS uptake by MCF-7 cells was determined using FACS Calibur flow cytometry (BD FACSCalibur, BD bioscience, CA, USA).

Cytotoxicity assessment

Cytotoxicity of ARI, NIOs, NIOs/ARI, NIOs/AuNPs-CS, and NIOs/AuNPs-CS/ARI on MCF-7 cells was evaluated by MTT assay. Cells at a density of 5×10^3/well were cultured in a 96-well plate. Following overnight culture, the cells were treated with 12, 24, 48, and 96 µM concentrations of ARI, NIOs, NIOs/ARI, NIOs/AuNPs-CS, and NIOs/AuNPs-CS/ARI. After 24 and 48 h of treatment, the media was removed, and MTT solution was added and then incubated for a further 4 h. Subsequently, the MTT solution was replaced by DMSO, and an ELISA reader (Elx808, BioTek Instruments, Winooski, VT, USA) at a wavelength of 570 nm was used to determine the absorbance.

Apoptosis/necrosis assessment

An Annexin V/PI apoptosis detection kit was utilized to examine the impact of ARI, NIOs, ARI/NIOs, NIOs/AuNPs-CS, and NIOs/AuNPs-CS/ARI with concentration of 48 µm on the apoptosis/necrosis of MCF-7 cells. To this end, 5×10^5 MCF-7 cells per well were seeded into 6-well plates. After 24 h, cells were treated with samples and then incubated for 48 h. Subsequently, the cells were washed, trypsinized, and centrifuged at 160 g for 5 minutes. After washing with PBS, cells were resuspended in binding buffer (100 µL), and then 10 µL of FITC-Annexin V and PI were added for staining. Samples were incubated at 4 °C for 10 min, then the cells were analyzed using FACS flow cytometry (BD FACSCalibur, BD bioscience, CA, USA).

The effect of hyperthermia on cytotoxicity

To determine the effects of ARI in combination with hyperthermia on cancer cells, MCF-7 cells were seeded in a 96-well plate with a density of 5×10^3 per well. After 24 h, cells were treated with ARI, NIOs, NIOs/ARI, NIOs/AuNPs-CS, and NIOs/AuNPs-CS/ARI at a concentration of 48 µM. After 4 h of treatment, the cells were exposed to the laser radiation (525 nm) (Mustang@ 2000, Russia) for 1 min. The cells were further cultured for 24, and 48 h, and then the MTT assay was performed.

Statistical analysis

In this study, each experiment was repeated at least three times, and the results were expressed as the mean±standard deviation (SD). ANOVA, a multiple comparison test involving three or more groups, was used to analyze the data and statistical significance was determined with a p-value less than 0.05. Prism, version 9.3, was used for all statistical analysis.

Results and discussion

NIOs possess distinctive properties that make them favorable drug delivery systems (DDSs). These include their ability to simultaneously load both hydrophilic and hydrophobic drugs, ease of synthesis, low toxicity, and biocompatibility [29]. In this study, our objective was to

engineer a suitable niosomal nanosystem for the combined chemo/photothermal therapy of breast cancer. Chitosan-coated AuNPs, as pH-responsive PTT agents were synthesized. Subsequently, ARI and AuNPs-CS were loaded in the hydrophobic domain and hydrophilic core of NIOs, respectively (Fig. 1). Then their physicochemical characteristics and biological impacts were studied in MCF-7 breast cancer cells.

NIOs/AuNPs-CS characterization

The particle size is a crucial factor in the development of nanotechnology-based DDSs. Recent advancements indicate that NPs with a size of about 50–100 nm have significant potential for cancer therapy [30]. Owing to a high rate of angiogenesis, solid tumors display abnormal leaky vasculature with an irregular shape and a lack of a smooth muscle layer. These characteristics can be harnessed to increase the NPs penetration from the blood circulation to the tumor tissues through enhanced permeability and retention (EPR) [31]. These characteristics make them highly advantageous for biomedical applications. The size of the prepared NIOs and NIOs/AuNPs-CS were 54.77, and 44.62 nm, respectively (Fig. 2a, c), as evaluated by dynamic light scattering. Previous research has demonstrated the high sensitivity of NIOs to aggregation. Following sonication, NIOs can exhibit significant aggregation [32, 33]. In our study, NIOs are slightly larger than NIOs/AuNPs-CS, which could be due to the aggregation of NIOs. In our previous study, it was also observed that the size of bare NIOs were larger than NIOs/AuNPs and NIOs/AuNPs-Polyamidoamine [34]. TEM and SEM analysis were performed for size and morphology assessment, which showed the prepared NIOs and NIOs/AuNPs-CS have a spherical shape with a size of around 50 nm for NIOs (Fig. 3a and c) and almost 38 nm for NIOs/AuNPs-CS (Fig. 3b). Morphological characterization of NIOs acquired by TEM and SEM analysis indicated a smaller size than the DLS measurement since the zeta sizer indicates the hydrated diameter form of NPs, which is consistently larger than NPs' accurate diameters [35]. Further, the zeta potential of NIOs/AuNPs-CS (-0.836) was found to be more neutral compared to NIOs (-14.8) (Fig. 2b, d), which can be attributed to the presence of CS. The positively charged amino groups of CS influence the zeta potential of the fabricated NPs [36]. NPs with a zeta potential of -10 to +10 mV and a size of less than 100 nm promote their function and enhance their qualities for DDSs [37, 38]. Therefore, the NIOs/AuNPs-CS have suitable size and zeta potential for biomedical applications.

FT-IR spectra were used to determine the chemical structure of NIOs, and NIOs/AuNPs-CS (Fig. 4a). The peaks identified were at 1738 cm^{-1} attributed to a 5-membered ring [39]. In the spectrum of NIOs/AuNPs-CS, the bands at 2900 cm^{-1} and 3400 cm^{-1} are related to the stretching vibrations of CH_2 and hydroxyl groups, respectively [40]. The peaks at 1382 and 1646 cm^{-1} are for C-N stretching and C=O amide stretching of CS, while 3417 cm^{-1}, and 1106 cm^{-1} could be related to the asymmetric stretch of C–O–C groups of CS and NIOs [41, 42]. The peak at 1580–1650 cm^{-1} is related to AuNPs-CS for the amines group of CS [43], which does not exist in bare NIOs. The characteristic peaks of 1457 cm^{-1} which indicate alkanes and the aromatic ring

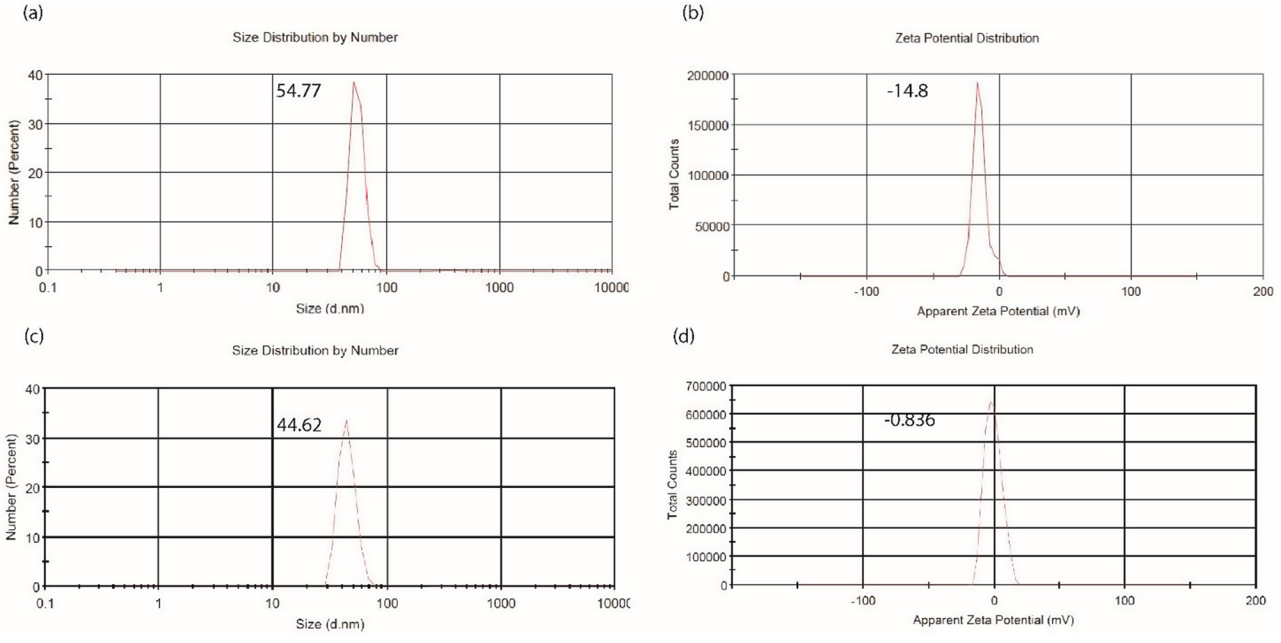

Fig. 2 The size (**a**, **c**) and zeta potential (**b**, **d**) distribution of NIOs and NIOs/AuNPs-CS respectively. Zeta potential of (**b**) NIOs, (**d**) NIOs/AuNPs-CS

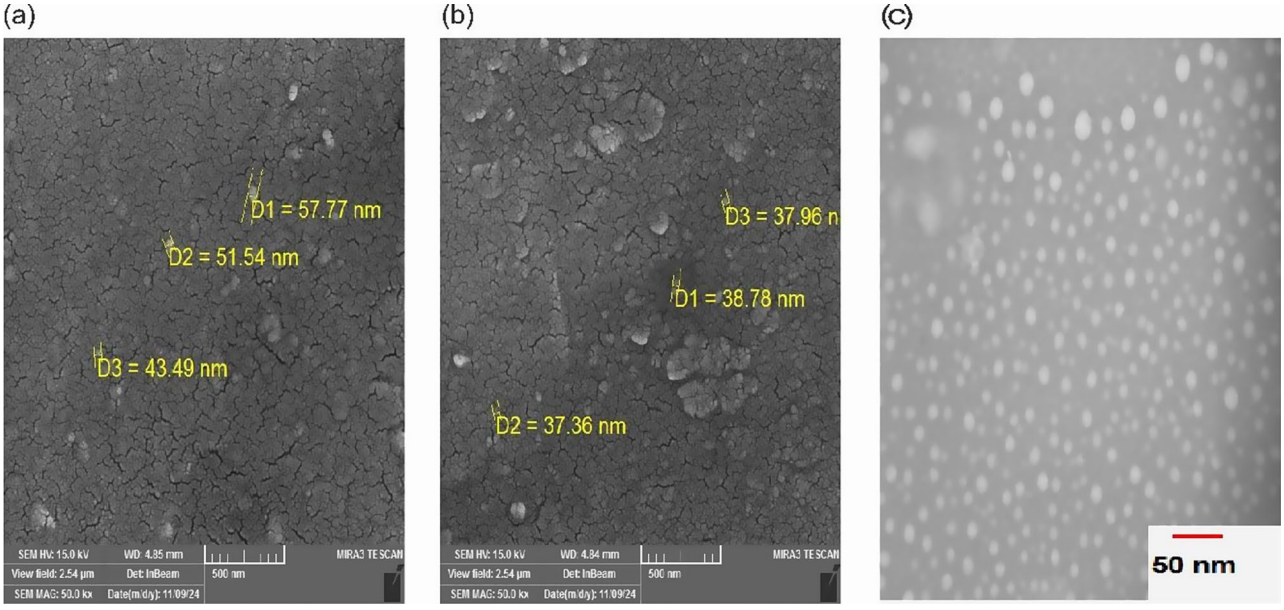

Fig. 3 The SEM images (scale bar = 2.54 µm) of (**a**) NIOs, (**b**) NIOs/AuNPs-CS, and (**c**) the TEM image of NIOs

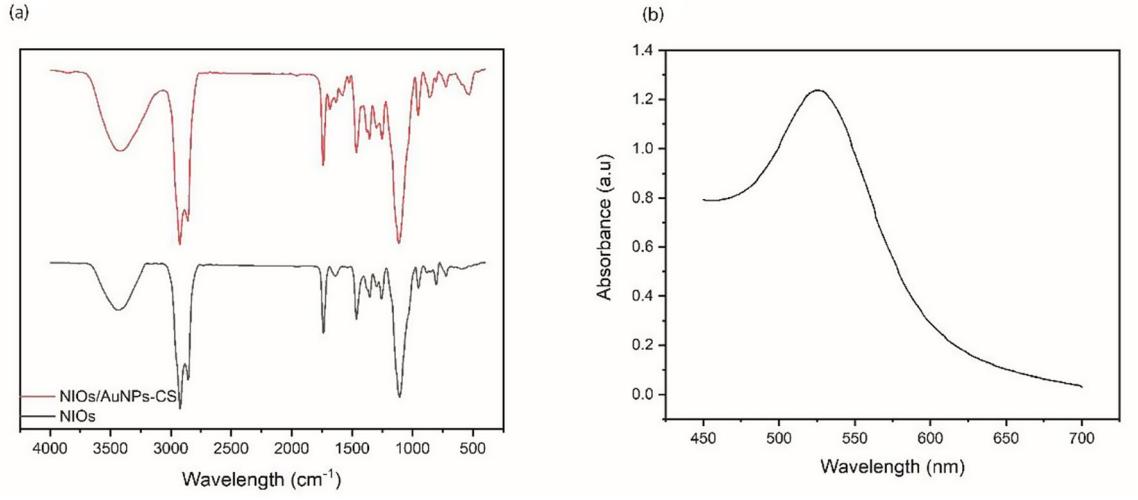

Fig. 4 (**a**) The FT-IR spectra of NIOs and NIOs/AuNPs-CS. (**b**) The UV-Vis spectrum of NIOs/AuNPs-CS

stretch functional group were found in Tween 80, cholesterol, and Span 60 [44]. The lipophilic region is chains made up of alkanes [45], which are similar in both NIOs and NIOs/AuNPs-CS indicating that AuNPs-CS did not interact in lipophilic regions. As shown in Fig. 4b, a clear and single peak at 525 nm was observed in the UV-Vis spectrum indicating that AuNPs-CS was successfully synthesized and can be used in PTT.

Drug entrapment efficiency drug release

As amphiphilic NPs, NIOs could entrap the hydrophobic and hydrophilic drugs simultaneously [46]. As previously demonstrated, NIOs exhibit a significant capability for carrying hydrophobic drugs such as paclitaxel, with remarkable %EE values of 98.5% [47]. In this study, NIOs/AuNPs-CS nanosystems were used for delivering ARI as a hydrophobic drug. The loading efficiency of ARI in simple NIOs and NIOs/AuNPs–CS was 75 and 84%, respectively, indicating excellent loading efficiency. The high drug loading in nanostructures can be attributed to span 60, characterized by its low hydrophobic moiety values, promoting the formation of robust and stable NIOs with exceptional entrapment efficiency [48]. Similarly, cholesterol is known to positively influence the permeability, rigidity, leakage, and entrapment efficiency of NIOs [49]. The synthesis of AuNPs using chitosan would improve its surface properties for binding of biomolecules which can increase drug loading efficiency [50].

Developing a smart nanocarrier with a high encapsulation efficiency, and regulated release property is a critical

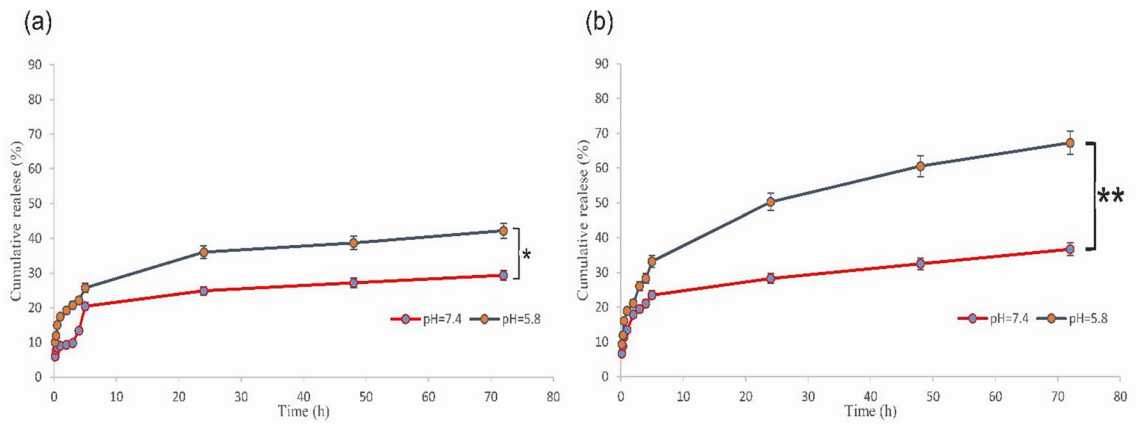

Fig. 5 The cumulative in vitro release of ARI from (**a**) NIOs and (**b**) NIOs/AuNPs-CS at pH = 7.4 and 5.8 at 37 °C, ∗, ∗∗ represented $p < 0.05$ and $p < 0.01$, respectively ($n = 3$)

Table 1 The kinetics models of ARI release from NIOs/ARI

Kinetics model	Equation	Coefficient of determination (R^2)	
		pH = 5.8	pH = 7.4
Zero-order	$F = k_0 t$	0.8576	0.7367
First order	$\ln(1-F) = -k_f t$	0.9322	0.7844
Higuchi	$F = k_H \sqrt{t}$	0.969	0.8811
Power law[a]	$\ln F = \ln k_P + P \ln t$	0.9903	0.9516
Square root of mass	$1 - \sqrt{1-F} = k_{1/2} t$	0.8977	0.7609
Hixson-Crowell	$1 - \sqrt[3]{1-F} = k_{1/3} t$	0.9099	0.7688
Three seconds' root of mass	$1 - \sqrt[3]{(1-F)^2} = k_{2/3} t$	0.8849	0.7529
Weibull[b]	$\ln(-\ln(1-F)) = -\beta \ln t_d + \beta \ln t$	0.9937	0.9618
Reciprocal powered time[c]	$\left(\frac{1}{F} - 1\right) = \frac{m}{t^b}$	0.9885	0.9701

[a] pH = 5.8: kP = 0.1645 and P = 0.2315; pH = 7.4: kP = 0.0955 and P = 0.2708

[b] pH = 5.8: β = 0.2661 and td = 615.2458; pH = 7.4: β = 0.2948 and td = 2391.1066

[c] pH = 5.8: m = 4.9973 and b = 0.3046; pH = 7.4: m = 9.3633 and b = 0.3204

challenge in cancer therapy [51]. On the other hand, the acidic tumor microenvironment (TME), primarily due to anaerobic glucose metabolism, presents an opportunity for developing intelligent, pH-driven, controlled-release DDSs [51]. Previous research has demonstrated that the hydrophobicity of tween 80 may favor the retention of hydrophobic drugs, such as ARI on the vesicle's surface rather than encapsulation within the system [48]. The decoration of AuNPs-CS on the surface of NIOs influences their pH sensitivity. This is due to the protonation of amino groups of CS under acidic conditions, thereby increasing their solubility and drug release [51]. Moreover, in previous research, the NIO formulation allowed for a more gradual release of ARI in physiological pH due to its lipophilicity, demonstrating the NIO's effectiveness in controlled drug delivery applications [52]. The cumulative in vitro release profile of ARI from formulated NIOs and NIOs/AuNPs-CS composite at pH=7.4 and 5.8 at 37 °C is shown in Fig. 5. The rates of ARI released from NIOs/AuNPs-CS are higher than NIOs in both pH conditions. These findings demonstrated that NIOs/AuNPs-CS possess unique pH-responsive drug release properties, making them a suitable smart DDS. Various kinetic models were employed to fit the release of ARI from NIOs/ARI and NIOs/AuNPs-CS/ARI as presented in Tables 1 and 2. The analysis indicated that at the pHs of 7.4 and 5.8, the release curves best fit with the Power law, Weibull, and Reciprocal powered time kinetic models (as shown in Tables 1 and 2) . The results of this study are consistent with our prior work, which demonstrated the release of silibinin from NIOs with similar behavior [53]. The Weibull and Power law release kinetics indicated the drug release profile is largely based on diffusion while swelling and erusion mechanisms might be somewhat involved since the biopolymer is subjected to degradation [54]. The Reciprocal powered time model also indicated a controlled release behavior [55]. Based on the release kinetics data, Power Law model seems to be a better fit for the drug release, in which the release exponent is smaller than 0.5, indicating the drug release is primarily governed by Fickian diffusion through the polymer matrix at both pHs. However, we speculate that upon the initial release of the

Table 2 The kinetics models of ARI release from NIOs/AuNPs-CS/ARI

Kinetics model	Equation	Coefficient of determination (R^2)	
		pH = 5.8	pH = 7.4
Zero-order	$F = k_0 t$	0.7917	0.7627
First order	$\ln(1-F) = -k_f t$	0.832	0.7845
Higuchi	$F = k_H \sqrt{t}$	0.7211	0.892
Power law[a]	$\ln F = \ln k_P + P \ln t$	0.9866	0.922
Square root of mass	$1 - \sqrt{1-F} = k_{1/2} t$	0.8123	0.7736
Hixson-Crowell	$1 - \sqrt[3]{1-F} = k_{1/3} t$	0.819	0.7773
Three seconds' root of mass	$1 - \sqrt[3]{(1-F)^2} = k_{2/3} t$	0.8055	0.77
Weibull[b]	$\ln(-\ln(1-F)) = -\beta \ln t_d + \beta \ln t$	0.99	0.9217
Reciprocal powered time[c]	$\left(\frac{1}{F} - 1\right) = \frac{m}{t^b}$	0.9913	0.9211

[a]pH = 5.8: *kP* = 0.1809 and *P* = 0.3186; pH = 7.4: *kP* = 0.1316 and *P* = 0.2623

[b]pH = 5.8: β = 0.3916 and *td* = 58.5851; pH = 7.4: β = 0.2917 and *td* = 798.3528

[c]pH = 5.8: *m* = 4.3540 and *b* = 0.4792; pH = 7.4: *m* = 6.4734 and *b* = 0.3237

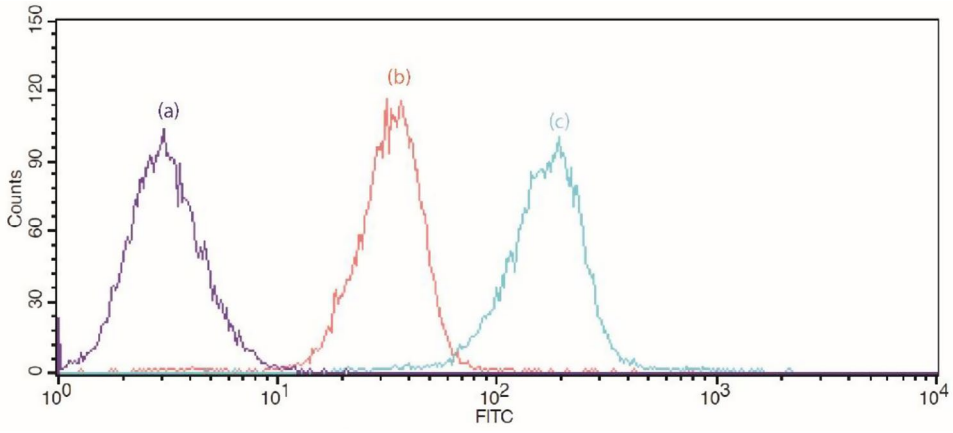

Fig. 6 Cellular uptake (a) untreated group, (b) NIOs, and (c) NIOs/AuNPs-CS

drugs, the polymer swelling and possible degradation process might be involved in drug release. Furthermore, based on Weibull kinetics model (with a shape parameter, b < 1), the rate of drug release decreases over time, which further indicates that drug release profile is largely dependent upon the diffusion phenomenon.

Cellular uptake

Cellular uptake of NPs plays a key role in assessing the efficacy of DDSs. Particle size, shape, and surface charge can influence the mechanism of cellular uptake and the efficiency of the therapeutic agent [56]. Previous studies have demonstrated that the uptake of different NPs by nonphagocytic cells is highly correlated to the size of NPs [57]. Uptake reaches an optimum level at around 50 nm, then declines for particles of higher sizes [58]. In addition, the shape of NPs directly influences cellular uptake, and spherical NPs show the highest uptake after rod-NPs [59]. Owing to the presence of phospholipids, the cell membrane has a slight negative charge, and cell uptake is driven by electrostatic attractions. Therefore, the positively charged NPs are taken up faster than negatively charged NPs [59, 60]. Figure 6 presents the uptake of NIOs and NIOs/AuNPs-CS by MCF-7 cancer cells. It was shown that NIOs can be transported into the cells because of their small size and sphere shape. However, cell uptake of NIOs/AuNPs-CS was significantly higher due to the positive charge of NIOs/AuNPs-CS compared to NIOs and enhanced cell membrane interaction with the particles.

Cell cytotoxicity evaluation by MTT assay

The MCF-7 cells were treated with free ARI, NIOs, ARI/NIOs, NIOs/AuNPs-CS, and NIOs/AuNPs-CS/ARI at concentrations of 12, 24, 48, and 96 μM for 24 and 48 h, and then the MTT assay was performed. As shown in Fig. 7, NIOs and NIOs/AuNP-CS formulations have negligible cytotoxicity against the MCF-7 cells. Such cytocompatibility is mainly attributed to the low cytotoxicity of the ester surfactants (span and tween) used to prepare NIOs, indicating the great potential of NIOs formulations for drug delivery applications [61]. Previous studies

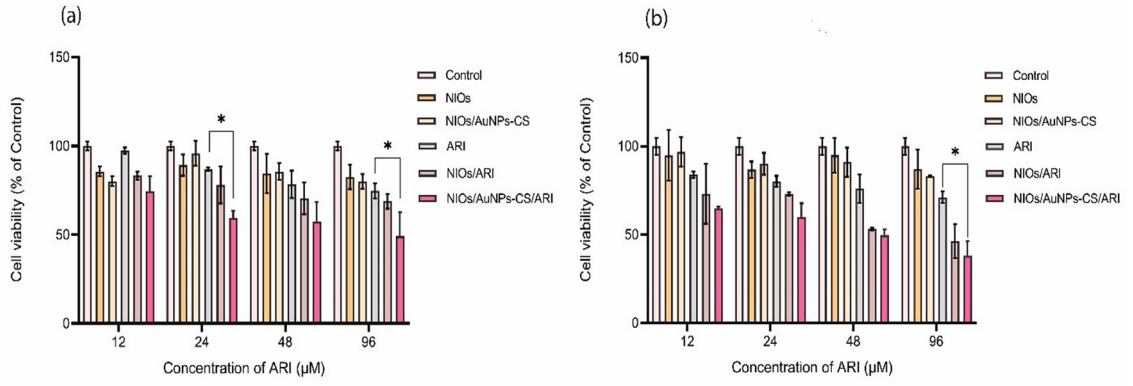

Fig. 7 The cytotoxicity of ARI, NIOs, NIOs/ARI, NIOs/AuNPs-CS, and NIOs/AuNPs-CS/ARI on the MCF-7 cells after (**a**) 24 h and (**b**) 48 h, $p^* < 0.05$, ($n = 4$)

have shown that ARI inhibits the proliferation of MCF-7 cells in a concentration-dependent manner [23]. However, some studies have indicated that free ARI exhibits relatively weaker effects in inhibiting cell proliferation when compared to its efficacy in combination with other agents, such as Cisplatin [26] and in some cancer cell lines, achieving the half-maximal inhibitory concentration (IC50) may require the use of very high concentrations of ARI (>100 μM) [62]. Our study has demonstrated that ARI-loaded NIOs exhibit higher cytotoxicity as compared to free ARI, due to increased solubility and subsequently enhanced intracellular levels in MCF-7 cells [63]. Moreover, targeted NPs can enter the target cells, through receptor-mediated endocytosis, increasing the concentration of drug molecules within the cell. During this process, P-gp does not recognize drug molecules and fails to pump out the free drug molecules from the cell [64]. Besides, in our latest studies, niosomal formulations were highly biocompatible, as there was no significant cytotoxicity on the HHF-2 and HEK-293 (normal cell lines) [35, 53]. NIOs/AuNPs-CS/ARI have more inhibitory effects on MCF-7 compared to NIOs/ARI (50% VS 53%, at the concentration of 48 μM after 48 h), which is not statistically significant ($p > 0.05$) between two groups. Since sample size and measurement variability can easily influence the statistical results, a nonsignificant outcome does not imply that the new therapy or treatment protocol is not clinically useful [65]. The reason for this slight increase may be due to the high uptake of NIOs/AuNPs-CS/ARI by MCF-7 cells [66]. The IC50 of ARI loaded in NPs was about 48 μM after 48 h. This concentration was used for the subsequent experiments and combination therapy step.

Flow cytometry assay

Studies have demonstrated that ARI increases the apoptosis rate in the various cancer cells by regulating the expression of key proapoptotic genes, such as BCL10 and caspases 3, along with anti-apoptotic genes like BCL2L1, and c-myc [23]. In various studies, loading drugs into almost the same nanoplatforms has shown significantly higher apoptosis rates in cancer cells compared to administering free drugs. For instance, a formulation of doxorubicin and vincristine loaded into CS-coated NIOs demonstrated a notable increase in apoptosis in cancer cells compared to the effects of free drugs [67]. Our latest study reported that loading paclitaxel onto NIOs/AuNPs-Polyamidoamine platform produced a higher apoptotic rate in cancer cells than free paclitaxel [34]. Our findings reveaedl that ARI (48 μM) loaded in a composite nanosystem of NIOs/AuNPs-CS significantly increases the apoptosis and necrosis rate, specifically in the cells treated with NIOs/AuNPs-CS/ARI reaching %46 after 48 h. This surpasses the corresponding rates observed with NIOs/ARI and free ARI, which are %36 and %26, respectively (Fig. 8). This observation may be attributed to enhanced cellular uptake facilitated by improved interaction with the cell membrane.

Combination therapy

The combined chemo/PTT therapeutic efficacy of drug-loaded NIOs and NIOs/AuNPs-CS on MCF-7 cancer cells was investigated after 24 and 48 h. These findings have shown that NIOs did not have cytotoxicity, while NIOs/AuNPs-CS have shown significant cytotoxicity. Previous studies have demonstrated that small gold nanospheres have negligible damage to the mitosis and DNA synthesis at normal growth temperature, while this defect was exacerbated by mild hyperthermia conditions [68]. Laser irradiation itself has also been shown to have no cytotoxic effects on the untreated cells (control +), because PTT works by exerting local cytotoxic hyperthermia on the treated cancer cells through a photothermal contrast agent. In this approach, a photothermal contrast agent is used to deliver radiation energy to the tumor tissue [69]. Local hyperthermia mediated by AuNPs induced by a mild PTT can result in the apoptosis/necrosis of

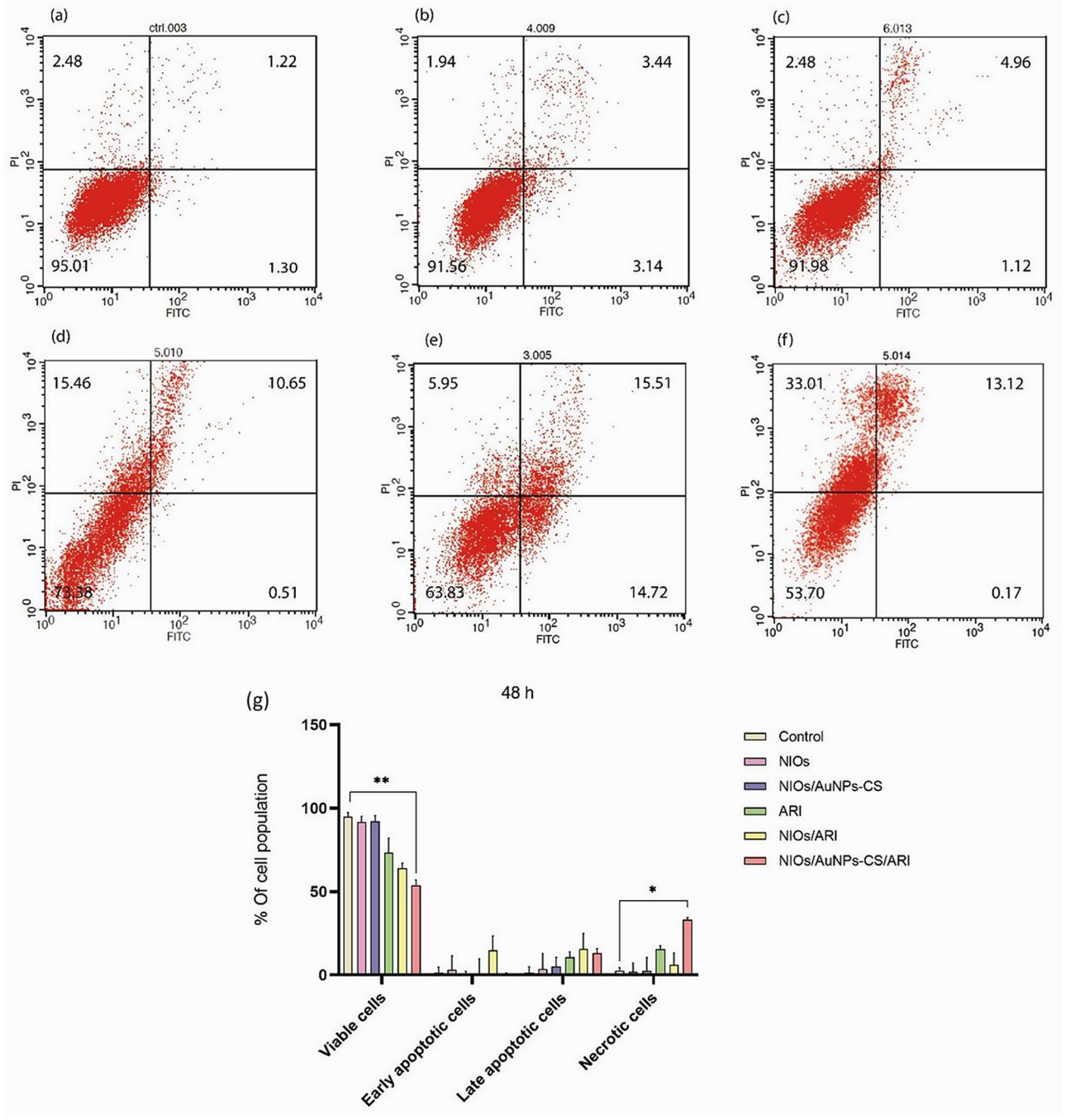

Fig. 8 Flow cytometry analysis of MCF-7 cells. (**a**–**f**) represents the cell population for the untreated control group and treated with NIOs, NIOs/AuNPs-CS, ARI, NIOs/ARI, and NIOs/AuNPs-CS/ARI after 48 h. (**g**) The viable, early apoptotic, late apoptotic, and necrotic cell population upon 48 h treatment. *, ** represented $p < 0.05$ and $p < 0.01$, respectively ($n = 2$)

cancer cells by denaturing proteins and enzymes, disrupting metabolic signals, and swelling the endothelium, among other effects [70]. Moreover, combination therapy decreases the IC50 in MCF-7 cells treated by NIOs/AuNPs-CS/ARI which IC50 has shown in 24 h. In contrast, at the same concentration, IC50 was observed at 48 h without PTT. Notably, the cytotoxicity of NIOs/AuNPs-CS/ARI with PTT was found to be substantial, resulting in a cell death rate of approximately 60% in 24 h and around 80% in 48 h (Fig. 9).

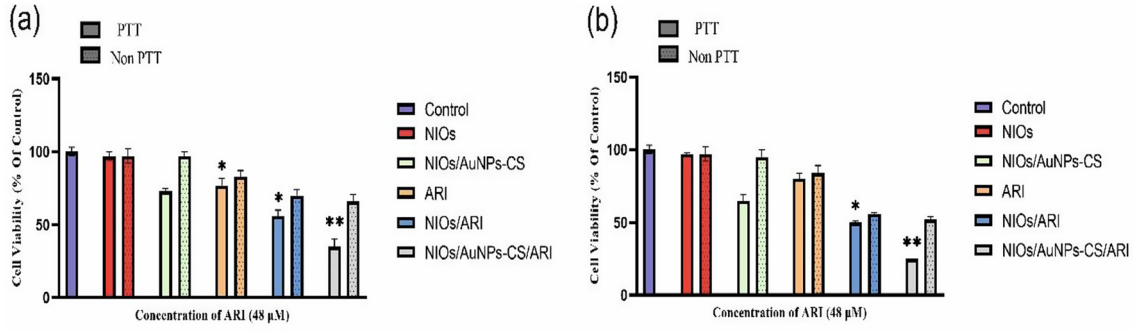

Fig. 9 The cytotoxicity of ARI, NIOs, NIOs/ARI, NIOs/AuNPs-CS, and NIOs/AuNPs-CS/ARI on the MCF-7 cells, with and without laser irradiation after (**a**) 24 and (**b**) 48 h, *, ** represented $p < 0.05$ and $p < 0.01$, respectively, ($n = 4$)

Conclusion

Transitioning from monotherapy to combination therapy for cancer presents numerous advantages, including reduced side effects with efficient eradication of cancer cells. In this research, we successfully synthesized and characterized NIOs/AuNPs-CS/ARI for breast cancer treatment. Considering the amphiphilic properties of NIOs, we loaded ARI into the hydrophobic core while decorating the surface with AuNPs-CS. The use of AuNPs for PTT serves to convert light into heat, thereby enhancing the effect of ARI against breast cancer cells. Furthermore, incorporating AuNPs-CS into the fabrication of DDS results in a positively charged surface for NIOs/AuNPs-CS, promoting uptake by cancer cells compared to NIOs. This research underscores the potential of NIOs/AuNPs-CS/ARI, with their unique properties, as a promising strategy for targeting breast cancer. Future investigations, including in vivo studies or the use of different ligands, could provide essential insights needed to advance this approach toward clinical trials. This combination therapy has the potential to integrate smoothly into existing breast cancer treatment protocols, improving patient survival by reducing side effects and addressing drug resistance.

Acknowledgements
The authors like to acknowledge the support provided by the Research Center for Pharmaceutical Nanotechnology (RCPN) at Tabriz University of Medical Sciences for both technical and financial support.

Author contributions
SM: Conceptualization; Methodology; Data curation; Formal analysis; Visualization; Original draft. MKZ: Conceptualization; Methodology; Data curation; Formal analysis; review & editing. PSP: Formal analysis. EDA: Formal analysis. JB: Conceptualization; review & editing. YO: Conceptualization; review & editing. MMP: Validation; Funding acquisition; Project administration. MF: Supervision; Validation; Visualization; Project administration. JS: Supervision; Validation; Project administration.

Funding
This study, as part of a DVM thesis, was supported by the Research Center for Pharmaceutical Nanotechnology, Tabriz University of Medical Sciences (Grant#68893).

Data availability
All data that support the findings of this study are included in the article.

Declarations

Ethical approval
This study was approved by the Research Ethics Committee of Tabriz University of Medical Sciences (IR.TBZMED.VCR.REC.1400.539).

Competing interests
The authors declare no competing interests.

Author details
[1]Research Center for Pharmaceutical Nanotechnology, Biomedicine Institute, Tabriz University of Medical Sciences, Tabriz, Iran
[2]Department of Basic Sciences, Faculty of Veterinary Medicine, Shabestar Branch, Islamic Azad University, Shabestar, Iran
[3]Department of Oral Science and Translation Research, College of Dental Medicine, Nova Southeastern University, Fort Lauderdale, FL 33313, USA
[4]Department of Pharmaceutical Sciences, College of Pharmacy, Nova Southeastern University, Fort Lauderdale, FL, USA
[5]Department of Reproductive Biology, Faculty of Advanced Medical Sciences, Tabriz University of Medical Sciences, Tabriz, Iran
[6]Engineered Biomaterial Research Center, Khazar University, Baku, Azerbaijan
[7]Department of Microbiology, Faculty of Veterinary and Agriculture, Islamic Azad University, Shabestar Branch, Shabestar, Iran

Received: 7 October 2024 / Accepted: 16 December 2024
Published online: 24 December 2024

References

1. Zenjanab MK, Alimohammadvand S, Doustmihan A, Kianian S, Oskouei BS, Mazloomi M, et al. Paclitaxel for breast cancer therapy: a review on effective drug combination modalities and nano drug delivery platforms. J Drug Deliv Sci Technol. 2024;95:105567.
2. Butti R, Das S, Gunasekaran VP, Yadav AS, Kumar D, Kundu GC. Receptor tyrosine kinases (RTKs) in breast cancer: signaling, therapeutic implications and challenges. Mol Cancer. 2018;17(1):1–18.
3. Jiang R-y, Zhu J-y, Zhang H-p, Yu Y, Dong Z-x, Zhou H-h, Wang X. STAT3: key targets of growth-promoting receptor positive breast cancer. Cancer Cell Int. 2024;24(1):356.
4. Persi E, Duran-Frigola M, Damaghi M, Roush WR, Aloy P, Cleveland JL, et al. Systems analysis of intracellular pH vulnerabilities for cancer therapy. Nat Commun. 2018;9(1):2997.
5. Burguin A, Diorio C, Durocher F. Breast cancer treatments: updates and new challenges. J Personalized Med. 2021;11(8):808.
6. Tian Y, Wang X, Wu C, Qiao J, Jin H, Li H. A protracted war against cancer drug resistance. Cancer Cell Int. 2024;24(1):326.

7. Alimohammadvand S, Zenjanab MK, Mashinchian M, Shayegh J, Jahanban-Esfahlan R. Recent advances in biomimetic cell membrane–camouflaged nanoparticles for cancer therapy. Biomed Pharmacother. 2024;177:116951.
8. Faid AH, Hussein FEZ, Mostafa EM, Shouman SA, Badr YA, Sliem MA. Hybrid chitosan gold nanoparticles for photothermal therapy and enhanced cytotoxic action of 6-mercaptopurine on breast cancer cell line. Beni-Suef Univ J Basic Appl Sci. 2023;12(1):83.
9. Liu J, Cabral H, Mi P. Nanocarriers address intracellular barriers for efficient drug delivery, overcoming drug resistance, subcellular targeting and controlled release. Adv Drug Deliv Rev. 2024;207:115239.
10. Rajera R, Nagpal K, Singh SK, Mishra DN. Niosomes: a controlled and novel drug delivery system. Biol Pharm Bull. 2011;34(7):945–53.
11. Zenjanab MK, Pakchin PS, Fathi M, Abdolahinian ED, Adibkia K. Niosomes containing paclitaxel and gold nanoparticles with different coating agents for efficient chemo/photothermal therapy of breast cancer. Biomed Mater. 2024;19(3).
12. Liga S, Paul C, Moacă E-A, Péter F, Niosomes. Composition, formulation techniques, and recent progress as Delivery systems in Cancer Therapy. Pharmaceutics. 2024;16(2):223.
13. Li Z, Chen Y, Yang Y, Yu Y, Zhang Y, Zhu D, et al. Recent advances in nanomaterials-based chemo-photothermal combination therapy for improving cancer treatment. Front Bioeng Biotechnol. 2019;7:293.
14. Pinho S, Ferreira-Gonçalves T, Lopes J, Amaral MN, Viana AS, Coelho JM, et al. A Step Forward for the treatment of localized prostate Cancer using gold nanoparticles combined with laser irradiation. Int J Mol Sci. 2024;25(8):4488.
15. Wu M, Xiao Y, Wu R, Lei J, Li T, Zheng Y. Aggregable gold nanoparticles for cancer photothermal therapy. J Mater Chem B. 2024;12:8048–61.
16. Ma Y, Tong S, Bao G, Gao C, Dai Z. Indocyanine green loaded SPIO nanoparticles with phospholipid-PEG coating for dual-modal imaging and photothermal therapy. Biomaterials. 2013;34(31):7706–14.
17. Cao Y, Yi J, Yang X, Liu L, Yu C, Huang Y, et al. Efficient cancer regression by a thermosensitive liposome for photoacoustic imaging-guided photothermal/chemo combinatorial therapy. Biomacromolecules. 2017;18(8):2306–14.
18. König K. Multiphoton microscopy in life sciences. J Microsc. 2000;200(2):83–104.
19. Patil T, Gambhir R, Vibhute A, Tiwari AP. Gold nanoparticles: synthesis methods, functionalization and biological applications. J Cluster Sci. 2023;34(2):705–25.
20. Georgeous J, AlSawaftah N, Abuwatfa WH, Husseini GA. Review of gold nanoparticles: synthesis, properties, shapes, Cellular Uptake, Targeting, Release mechanisms and Applications in Drug Delivery and Therapy. Pharmaceutics. 2024;16(10):1332.
21. Fathi M, Alami-Milani M, Geranmayeh MH, Barar J, Erfan-Niya H, Omidi Y. Dual thermo-and pH-sensitive injectable hydrogels of chitosan/(poly (N-isopropylacrylamide-co-itaconic acid)) for doxorubicin delivery in breast cancer. Int J Biol Macromol. 2019;128:957–64.
22. Mohi-ud-din R, Chawla A, Sharma P, Mir PA, Potoo FH, Reiner Ž, et al. Repurposing approved non-oncology drugs for cancer therapy: a comprehensive review of mechanisms, efficacy, and clinical prospects. Eur J Med Res. 2023;28(1):345.
23. Badran A, Tul-Wahab A, Zafar H, Mohammad N, Imad R, Ashfaq Khan M, et al. Antipsychotics drug aripiprazole as a lead against breast cancer cell line (MCF-7) in vitro. PLoS ONE. 2020;15(8):e0235676.
24. Suzuki S, Okada M, Kuramoto K, Takeda H, Sakaki H, Watarai H, et al. Aripiprazole, an antipsychotic and partial dopamine agonist, inhibits cancer stem cells and reverses chemoresistance. Anticancer Res. 2016;36(10):5153–61.
25. Jiang C, Lee SH, Park JH, Lee J-S, Park JW, Kim JR, et al. A low dose of aripiprazole has the strongest sensitization effect among 19 repositioned bipolar drugs in P-gp-overexpressing drug-resistant cancer cells. Anticancer Res. 2021;41(2):687–97.
26. Cho YJ, Han BS, Ko S, Park MS, Lee YJ, Kim SE, et al. Repositioning of aripiprazole, an anti–psychotic drug, to sensitize the chemotherapy of pancreatic cancer. Int J Mol Med. 2025;55(1):1–13.
27. Aslzad S, Heydari P, Abdolahinia ED, Amiryaghoubi N, Safary A, Fathi M, Erfan-Niya H. Chitosan/gelatin hybrid nanogel containing doxorubicin as enzyme-responsive drug delivery system for breast cancer treatment. Colloid Polym Sci. 2023;301(3):273–81.
28. Thabet Y, Elsabahy M, Eissa NG. Methods for preparation of niosomes: a focus on thin-film hydration method. Methods. 2022;199:9–15.
29. Muzzalupo R, Tavano L. Niosomal drug delivery for transdermal targeting: recent advances. Res Rep Trenasderm Drug Deliv. 2015;4:23–33.
30. Cho K, Wang X, Nie S, Chen Z, Shin DM. Therapeutic nanoparticles for drug delivery in cancer. Clin Cancer Res. 2008;14(5):1310–6.
31. Jahanban-Esfahlan R, de la Guardia M, Ahmadi D, Yousefi B. Modulating tumor hypoxia by nanomedicine for effective cancer therapy. J Cell Physiol. 2018;233(3):2019–31.
32. Shahbazi R, Jafari-Gharabaghlou D, Mirjafary Z, Saeidian H, Zarghami N. Design and optimization various formulations of PEGylated niosomal nanoparticles loaded with phytochemical agents: potential anti-cancer effects against human lung cancer cells. Pharmacol Rep. 2023;75(2):442–55.
33. Bakand A, Moghaddam SV, Naseroleslami M, André H, Mousavi-Niri N, Alizadeh E. Efficient targeting of HIF-1α mediated by YC-1 and PX-12 encapsulated niosomes: potential application in colon cancer therapy. J Biol Eng. 2023;17(1):58.
34. Zenjanab MK, Pakchin PS, Fathi M, Abdolahinia ED, Adibkia K. Niosomes containing paclitaxel and gold nanoparticles with different coating agents for efficient chemo/photothermal therapy of breast cancer. Biomed Mater. 2024;19(3):035015.
35. Kaveh Zenjanab M, Abdolahinia ED, Alizadeh E, Hamishehkar H, Shahbazi R, Ranjbar-Navazi Z, et al. Hyaluronic acid-targeted niosomes for effective breast cancer chemostarvation therapy. ACS Omega. 2024;9(9):10875–85.
36. Xue M, Hu S, Lu Y, Zhang Y, Jiang X, An S, et al. Development of chitosan nanoparticles as drug delivery system for a prototype capsid inhibitor. Int J Pharm. 2015;495(2):771–82.
37. Surapaneni SK, Bashir S, Tikoo K. Gold nanoparticles-induced cytotoxicity in triple negative breast cancer involves different epigenetic alterations depending upon the surface charge. Sci Rep. 2018;8(1):12295.
38. Mushtaq A, Li L, Grøndahl L. Chitosan nanomedicine in cancer therapy: targeted delivery and cellular uptake. Macromol Biosci. 2021;21(5):2100005.
39. Khan MI, Madni A, Ahmad S, Khan A, Rehmanand M, Mahmood MA. ATR-FTIR based pre and post formulation compatibility studies for the design of niosomal drug delivery system containing nonionic amphiphiles and chondroprotective drug. J Chem Soc Pak. 2015;37(3).
40. Zarepour A, Egil AC, Cokol Cakmak M, Esmaeili Rad M, Cetin Y, Aydinlik S, et al. Fabrication of a dual-drug-loaded smart niosome-g-chitosan polymeric platform for lung cancer treatment. Polymers. 2023;15(2):298.
41. Mehta S, Jindal N. Formulation of Tyloxapol niosomes for encapsulation, stabilization and dissolution of anti-tubercular drugs. Colloids Surf B. 2013;101:434–41.
42. Samed N, Sharma V, Sundaramurthy A. Hydrogen bonded niosomes for encapsulation and release of hydrophilic and hydrophobic anti-diabetic drugs: an efficient system for oral anti-diabetic formulation. Appl Surf Sci. 2018;449:567–73.
43. Pakchin PS, Fathi M, Ghanbari H, Saber R, Omidi Y. A novel electrochemical immunosensor for ultrasensitive detection of CA125 in ovarian cancer. Biosens Bioelectron. 2020;153:112029.
44. Rehman MU, Rasul A, Khan MI, Hanif M, Aamir MN, Waqas MK, et al. Development of niosomal formulations loaded with cyclosporine A and evaluation of its compatibility. Trop J Pharm Res. 2018;17(8):1457–64.
45. Li D. Development and evaluation of a niosome carrier for topical use of antioxidant. ResearchSpace@ Auckland; 2014.
46. Mishra V, Nayak P, Singh M, Sriram P, Suttee A. Niosomes: potential nanocarriers for drug delivery. J Pharm Clin Res. 2020;11(03):389–94.
47. Kaveh Zenjanab M, Abdolahinia ED, Alizadeh E, Hamishehkar H, Shahbazi R, Ranjbar-Navazi Z, et al. Hyaluronic acid-targeted niosomes for effective breast cancer chemostarvation therapy. ACS Omega. 2024;9(9):10875–85.
48. Mawazi SM, Ann TJ, Widodo RT. Application of Niosomes in cosmetics: a systematic review. Cosmetics. 2022;9(6):127.
49. Moghtaderi M, Sedaghatnia K, Bourbour M, Fatemizadeh M, Salehi Moghaddam Z, Hejabi F, et al. Niosomes: a novel targeted drug delivery system for cancer. Med Oncol. 2022;39(12):240.
50. Bhumkar DR, Joshi HM, Sastry M, Pokharkar VB. Chitosan Reduced Gold Nanoparticles as Novel Carriers for Transmucosal Delivery of insulin. Pharm Res. 2007;24(8):1415–26.
51. Rostami E. Progresses in targeted drug delivery systems using chitosan nanoparticles in cancer therapy: a mini-review. Int J Drug Deliv Technol. 2020;58:101813.
52. Misal1a PS, Nawale SD, Shirbhate M. Preparation, optimization, compatibility study, and evaluation of in-vitro and in-vivo release study of aripiprazole pronisome. J Cardiovasc Dis Res. 2023;14(8):64–81.
53. Shafiei G, Jafari-Gharabaghlou D, Farhoudi-Sefidan-Jadid M, Alizadeh E, Fathi M, Zarghami N. Targeted delivery of silibinin via magnetic niosomal

nanoparticles: potential application in treatment of colon cancer cells. Front Pharmacol. 2023;14:1174120.
54. Barzegar-Jalali M. Kinetic analysis of drug release from nanoparticles. J Pharm Pharm Sci. 2008;11(1):167–77.
55. Herdiana Y, Wathoni N, Shamsuddin S, Muchtaridi M. Drug release study of the chitosan-based nanoparticles. Heliyon. 2022;8(1).
56. He C, Hu Y, Yin L, Tang C, Yin C. Effects of particle size and surface charge on cellular uptake and biodistribution of polymeric nanoparticles. Biomaterials. 2010;31(13):3657–66.
57. Chithrani BD, Ghazani AA, Chan WC. Determining the size and shape dependence of gold nanoparticle uptake into mammalian cells. Nano Lett. 2006;6(4):662–8.
58. Kettler K, Veltman K, van De Meent D, van Wezel A, Hendriks AJ. Cellular uptake of nanoparticles as determined by particle properties, experimental conditions, and cell type. Environ Toxicol Chem. 2014;33(3):481–92.
59. Albanese A, Tang PS, Chan WC. The effect of nanoparticle size, shape, and surface chemistry on biological systems. Annu Rev Biomed Eng. 2012;14:1–16.
60. Wang J, Tian S, Petros RA, Napier ME, DeSimone JM. The complex role of multivalency in nanoparticles targeting the transferrin receptor for cancer therapies. J Am Chem Soc. 2010;132(32):11306–13.
61. Ghafelehbashi R, Akbarzadeh I, Yaraki MT, Lajevardi A, Fatemizadeh M, Saremi LH. Preparation, physicochemical properties, in vitro evaluation and release behavior of cephalexin-loaded niosomes. Int J Pharm. 2019;569:118580.
62. Kim MS, Yoo BC, Yang WS, Han SY, Jeong D, Song JM, et al. Src is the primary target of aripiprazole, an atypical antipsychotic drug, in its anti-tumor action. Oncotarget. 2018;9(5):5979.
63. Abdelkader H, Alani AW, Alany RG. Recent advances in non-ionic surfactant vesicles (niosomes): self-assembly, fabrication, characterization, drug delivery applications and limitations. Drug Deliv. 2014;21(2):87–100.
64. Wang J, Wang F, Li F, Zhang W, Shen Y, Zhou D, Guo S. A multifunctional poly (curcumin) nanomedicine for dual-modal targeted delivery, intracellular responsive release, dual-drug treatment and imaging of multidrug resistant cancer cells. J Mater Chem B. 2016;4(17):2954–62.
65. Sharma H. Statistical significance or clinical significance? A researcher's dilemma for appropriate interpretation of research results. Saudi J Anaesth. 2021;15(4):431–4.
66. Aguilar A, Zein N, Harmouch E, Hafdi B, Bornert F, Offner D, et al. Application of chitosan in bone and dental engineering. Molecules. 2019;24(16):3009.
67. Karimifard S, Rezaei N, Jamshidifar E, Moradi Falah Langeroodi S, Abdihaji M, Mansouri A, et al. pH-Responsive Chitosan-Adorned Niosome Nanocarriers for Co-delivery of drugs for breast Cancer therapy. ACS Appl Nano Mater. 2022;5(7):8811–25.
68. Kodiha M, Hutter E, Boridy S, Juhas M, Maysinger D, Stochaj U. Gold nanoparticles induce nuclear damage in breast cancer cells, which is further amplified by hyperthermia. Cell Mol Life Sci. 2014;71:4259–73.
69. Dreaden EC, Mackey MA, Huang X, Kang B, El-Sayed MA. Beating cancer in multiple ways using nanogold. Chem Soc Rev. 2011;40(7):3391–404.
70. Zhang X. Gold nanoparticles: recent advances in the biomedical applications. Cell Biochem Biophys. 2015;72:771–5.

Publisher's note